

PAPER • OPEN ACCESS

Modified Scheil equation for the Cu-Sn system and comparison of hardness and electrical conductivity of Cu-8.5wt% Sn alloy directionally solidified

To cite this article: R A Cruz *et al* 2022 *IOP Conf. Ser.: Mater. Sci. Eng.* **1222** 012014

View the [article online](#) for updates and enhancements.

You may also like

- [Thermodynamic reassessment of Au-Pt-Sn system](#)
Jieqiong Hu, Ming Xie, Yongtai Chen et al.
- [Wafer level hermetic packaging based on Cu-Sn isothermal solidification technology](#)
Cao Yuhan and Luo Le
- [Transient liquid-phase sintering using silver and tin powder mixture for die bonding](#)
Masahisa Fujino, Hirozumi Narusawa, Yuzuru Kuramochi et al.



The Electrochemical Society
Advancing solid state & electrochemical science & technology

242nd ECS Meeting

Oct 9 – 13, 2022 • Atlanta, GA, US

Abstract submission deadline: **April 8, 2022**

Connect. Engage. Champion. Empower. Accelerate.

MOVE SCIENCE FORWARD



Submit your abstract



Modified Scheil equation for the Cu-Sn system and comparison of hardness and electrical conductivity of Cu-8.5wt% Sn alloy directionally solidified

R A Cruz^{1,2}, G A Santos¹, M S Nascimento¹, R Teram^{1,2}, R de Luca^{1,4}, V T dos Santos^{2,4}, M R da Silva⁴ and A A Couto^{2,3}

¹Federal Institute of Education, Science and Technology of São Paulo, São Paulo, SP, Brazil

²Mackenzie Presbyterian University, São Paulo, SP, Brazil

³Institute of Nuclear and Energy Research, IPEN, São Paulo, SP, Brazil

⁴Termomecanica São Paulo S.A., São Bernardo do Campo, SP, Brazil

ricardoapcruz@ifsp.edu.br

Abstract. The Scheil equation, which estimates the concentration of solute in the solid at the solid/liquid interface, does not account for the curvatures of *liquidus* and *solidus* lines. We modified the equation to account for these curvatures and compared some microsegregation indexes obtained by the original and the new equations with data from the literature about the Cu-Sn system. The new one can furnish a better approximation of the range of concentration of solute, but a poorer estimate of the maximum volume fraction of the eutectoid mixture. At last, we compared the hardness and electrical conductivity of an upward solidified alloy of this system with its equivalent commercial one. The as-cast alloy has a lower hardness and a higher conductivity due to its columnar structure.

1. Introduction

Microsegregation is a physical-chemical phenomenon. It occurs at the microstructural level during the solidification of an alloy. The difference in solubility for solute elements in the solid phase and the liquid phase drives that phenomenon. Under most solidification conditions, equilibrium can exist at the solid/liquid interface, and the concentrations of solid, C_S , and liquid, C_L , for any given element at the interface, can be used to define a partition ratio, k :

$$k = \frac{C_L}{C_{Si}} \quad (1)$$

C is concentration; subscripts S and L indicate solid and liquid, respectively; and subscript i indicates a quantity at the solid/liquid interface.

The Scheil equation estimates the concentration of solute in the solid at the solid/liquid interface. It assumes complete diffusion of solute in the liquid and zero diffusion in the solid, and can be written as follows [1].

$$C_{Si} = kC_0(1 - f_S)^{k-1} \quad (2)$$



C_0 is overall alloy concentration, and f_s is volume fraction of solid.

The partition ratio k seems to be not constant since the *liquidus* and *solidus* lines of the Cu-Sn phase diagram are not straight lines. It is necessary to correct this distortion, and we propose a new model to modify Scheil equations appropriately.

We will compare the original Scheil equations with the new ones by estimating some microsegregation indexes, such as the maximum volume fraction of the eutectoid mixture for three different alloys of the Cu-Sn system. We will also compare the hardness and electrical conductivity of an alloy of this system (Cu-8.5wt%Sn) subjected to upward solidification with the equivalent commercial one.

2. Proposed Model

Exists a quadratic function that can suitably relate C_{Si} to C_L and the curvature of the *solidus* line to the *liquidus* line. Using three pairs of points at different temperatures, and solving a system of three equations, we get [2]:

$$C_{Si} = 1.5986C_L^2 + 0.1218C_L \tag{3}$$

Equating the amount of solute that passed from the solid into the liquid, we get:

$$(C_L - C_{Si})df_s = (1 - f_s)dC_L \tag{4}$$

Supposing that an increase in the volume of solid implies an equal decrease in liquid ($df_s = -df_L$), the solving of equations (3) and (4) for the concentration of solute in the liquid phase will give:

$$C_L = \frac{-0.8782C_0}{1.5986C_0((1 - f_s)^{0.8782} - 1) - 0.8782(1 - f_s)^{0.8782}} \tag{5}$$

If we substitute (5) in (3), we will get the concentration of solute in the solid interface S/L. See in figure 1 the representation of Scheil equations and the new model equations for concentration of solute (Sn) in liquid and in solid interface as functions of the solid volume fraction ($C_0 = 8\text{wt\% Sn}$).

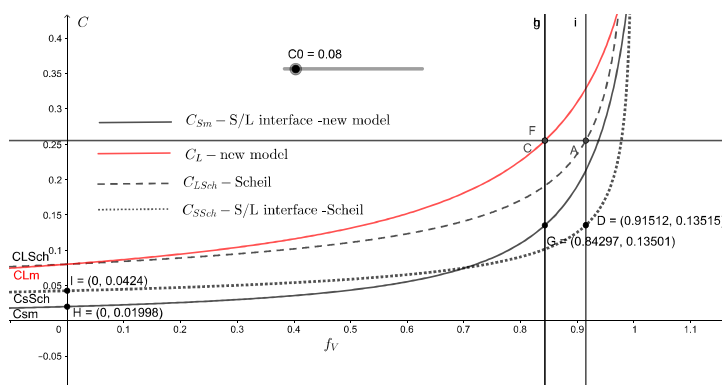


Figure 1. Representation of Scheil equations, (1) and (3), and of the new model equations, (3) and (5)

The area over the C_s function in the interval $0 \leq f_s \leq 1$ is equal to C_0 as to Scheil as to the new model, what indicates that there is mass conservation in both models.

3. Materials and Methods

We made the Cu-8.5wt% Sn alloy with commercially pure tin and UNS C50700 bronze. The melting of the material occurred in an electric furnace under an argon gas atmosphere. The solidification of the alloy occurred inside an upwardly unidirectional solidifying device. Thermocouples, a data acquisition system, and a computer allowed monitoring the temperature in eight sites of the cylindrical casting. More details of this technique is found in the literature [2-4].

We have cut the as-cast cylinder into samples. The sample destined for macrograph (half of the cylindrical casting from a longitudinal cut) was ground, polished, and etched with an acidic ferric chloride solution. Later, we measured electrical conductivity at five different distances from the base of that sample. The central part of the other half of the cylindrical casting gave rise to twelve transverse and twelve longitudinal samples taken from different distances from the base. They were embedded in pairs resulting in six bakelite disks for micrograph and six other disks for chemical analysis and hardness testing.

An inverted platinum microscope was used in conjunction with its software for digital image processing and analysis to make the necessary micrographs. We measured the primary and secondary dendrite arm spacing on the micrographs and proceeded to the statistical analysis of the distribution. The Manual Point Count Method allowed determining the volume fraction of the eutectoid mixture in each transverse sample [2,5,6].

We performed the Vickers hardness testing (HV10) on the six transverse and six longitudinal samples. Optical Emission Spectroscopy enabled the chemical analysis of the transverse samples.

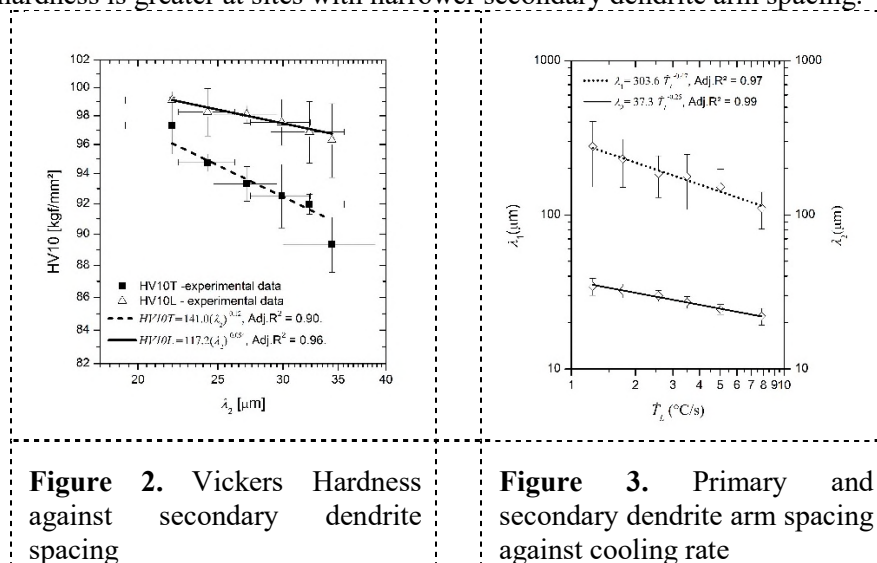
We used a DC10 electrical conductivity meter in a Wheatstone bridge circuit to measure the electrical conductivity in % IACS (International Annealed Copper Standard), according to the ASTM B193 standard.

4. Results and Discussion

The solidification produced a cylindrical casting about 115 mm high after deburring and cleaning. The macrostructure of this casting presented a columnar zone of about 80 mm in length. The analysis of the chemical composition of the transverse samples showed that there was no significant macrosegregation of tin along the height of the casting. The average mass fraction of tin was $(8.56 \pm 0.05)\text{wt}\%$ Sn.

4.1. Hardness HV10, dendrite arm spacing and cooling rate

Figure 2 shows the data of hardness in transversal and longitudinal samples plotted against the secondary dendrite arm spacing. Figure 3 displays the dendrite arm spacing plotted against the cooling rate. We note that the hardness is greater at sites with narrower secondary dendrite arm spacing.



A commercial alloy with 8.5%wt Sn (4.9%at Sn) would have a hardness of 128 HV for a grain size of 35 μm (OS035). See figure 4 to check the hardness of commercial alloys as a function of the atomic percentage of tin. The columnar morphology of the alloy obtained in the experiment produced a softer material in comparison with the commercial alloys, the maximum hardness value (98 HV10) is smaller than 128 HV (commercial).

4.2. Electrical conductivity

The electrical conductivity of the material after the solidification process is the same in any site. After five readings, we got the mean value: 14.4 ± 0.3 % IACS.

A commercial alloy with 8.5%wt Sn (4.9%at Sn) would have a resistivity of 139 n Ωm . See figure 5 to estimate the resistivity of commercial alloys. Therefore the corresponding conductivity of the commercial alloy is 12.4 % IACS. The columnar morphology of the alloy obtained in the experiment is responsible for a material with better conductivity (an increase of 16%) in comparison with the commercial alloys.

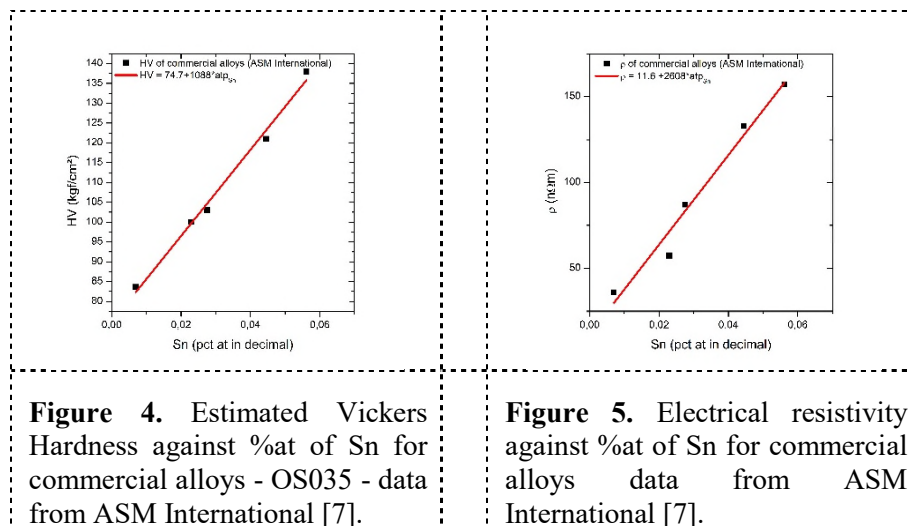


Figure 4. Estimated Vickers Hardness against %at of Sn for commercial alloys - OS035 - data from ASM International [7].

Figure 5. Electrical resistivity against %at of Sn for commercial alloys data from ASM International [7].

4.3. Volume fraction of the eutectoid mixture

The volume fraction of the eutectoid mixture varies from 0.9% to 2.6%. The mean value is 1.5%, and the standard deviation is 0.6%.

We found in the literature that the columnar morphology is associated with low values of volume fraction of eutectoid mixture in comparison to equiaxed morphology [6]. The theoretical maximum value for Vv in Cu-8.5%wtSn alloy is 9.7% (Scheil), and 17% (New model). Both values are by far superior in comparison with the maximum 2.6% measured. One can obtain the theoretical maximum value in this way: During the solidification of an alloy of the Cu-Sn system, the liquid becomes richer in Sn. When the concentration of solute in the liquid reaches 0.255 (25.5%) at the peritectic point, the remnant liquid will form a eutectoid mixture. The C_L equation can furnish us with the value of f_S when $C_L = 0.255$. If we subtract this value from 1, we will get the theoretical maximum value of the eutectoid mixture.

Table 5 displays some microsegregation data from the literature in comparison with the predictions of Scheil equation and the ones of the new model (NM) equation. The C_S range can be found substituting $f_S = 0$ and f_S of the peritectic point in C_{Si} equations, (2), (3) and (5).

Table 1. Comparison of some experimental data with the predictions of Scheil equations and of the new model (NM) equations.

	C ₀ (%wt)	Cs Exp. Range (%wt)	Cs Scheil Range (%wt)	Cs NM Range (%wt)	Vv exp. Range (%)	Scheil Vv (%)	NM Vv (%)	Observed Morphology
Ref. [6]	8	1.7-14.7	4.2-13.5	2-13.5	0.21-10.8	9.5	15.7	Col. ^a , eq. ^b
Ref. [8]	10	2-16	5.3-13.5	2.8-13.5	6-10.9	13.6	21.3	Eq.
Ref. [9]	20	6.5-13	10.6-13.5	8.8-13.5	20 (max)	59.7	62.4	Col.

^a Columnar^b Equiaxed

We can observe that NM equations give a better estimate of the Cs range, while Scheil equations provide a better estimate of the maximum volume fraction of the eutectoid mixture.

5. Conclusions

We can draw the following conclusions:

- (1) The modified Scheil equations provide a better estimate of the range of the mass fraction of solute in the solid and a poorer estimate of the maximum volume fraction of the eutectoid mixture.
- (2) The upward solidified alloy, with columnar structure, presented better conductivity (an increase of 16%) and lower hardness when compared to the equivalent commercial alloy.
- (3) The upward solidified alloy, with a columnar structure, presented a low value of eutectoid mixture in comparison with the estimates of the original Scheil equations and the new ones.

Acknowledgments

The authors are grateful for the support provided by CAPES, Salvador Arena Foundation Educational Center, Termomecanica São Paulo S.A., Mackenzie Presbyterian University, Nuclear and Energy Research Institute, and Federal Institute of São Paulo (IFSP) for the research activities.

References

- [1] Smith R. Microsegregation Measurement: Methods and Applications. Metall Mater Trans B Process Metall Mater Process Sci [Internet]. 2018;49(6):3258–79. Available at: <https://doi.org/10.1007/s11663-018-1395-4>
- [2] Cruz RA, Santos GA, Nascimento MS, Frajuca C, Nakamoto FY, da Silva MR, et al. Microstructural characterization and mathematical modeling for determination of volume fraction of eutectoid mixture of the cu-8.5wt% sn alloy obtained by unidirectional upward solidification. Mater Sci Forum. 2020;1012 MSF:302–7. Available at: <https://doi.org/10.4028/www.scientific.net/MSF.1012.302>
- [3] Nascimento M S, dos Santos G A, Teram R, dos Santos V T, da Silva M R, Couto A A. Effects of thermal variables of solidification on the microstructure, hardness, and microhardness of Cu-Al-Ni-Fe alloys. Materials (Basel). 2019;12(8). Available at: <https://doi.org/10.3390/ma12081267>
- [4] Nascimento MS, Tadeu ATR, Frajuca C, Yastami FY, dos Santos GA, Couto AA. An Experimental Study of the Solidification Thermal Parameters Influence upon Microstructure and Mechanical Properties of Al-Si-Cu Alloys. Materials Research 2018;21(5). Available at: <https://doi.org/10.1590/1980-5373-MR-2017-0864>
- [5] Kumoto E A, Alhadeff R O, Martorano M A. Microsegregation and dendrite arm coarsening in tin bronze. Mater Sci Technol. 2002;18(9):1001–6.
- [6] Martorano M de A, Capocchi J D T. Effects of Processing Variables on the Microsegregation of Directionally Cast Samples. Metallurgical Mater Trans A. 31A:3137–48.
- [7] ASM International. Metals HandBook VOL 2, Properties and Selection: Nonferrous Alloys and Special-Purpose Materials. 1990.
- [8] Kumoto EA, Alhadeff R O, Martorano MA. Microsegregation and dendrite arm coarsening in tin bronze. Mater Sci Technol. 2002;18:1001–6.

[9] Baptista LADS, Parabela KG, Ferreira IL, Garcia A, Ferreira AF. Experimental study of the evolution of tertiary dendritic arms and microsegregation in directionally solidified Al-Si-Cu alloys castings. *J Mater Res Technol* [Internet]. 2019;8(1):1515–21. Available at: <https://doi.org/10.1016/j.jmrt.2018.05.021>